Available online at www.sciencedirect.com
SCIENCE DIRECT®
ELSEVIER
Dyes and Pigments 69 (2006) 22–30
DYES and PIGMENTS
www.elsevier.com/locate/dyepig

Sol–gel derived silver doped nanocrystalline titania catalysed photodegradation of methylene blue from aqueous solution

S. Senthilkumaar*, K. Porkodi, R. Gomathi, A. Geetha Maheswari, N. Manonmani

Department of Chemistry, Faculty of Engineering, PSG College of Technology, Coimbatore-641 004, India

Received 13 October 2004; received in revised form 11 December 2004; accepted 21 February 2005
Available online 26 April 2005

Abstract

Nanocrstalline pure anatase titania doped with silver was prepared by sol–gel process at room temperature followed by ultrasonication (Ti–Ag–US). The photocatalytic activity of Ti–Ag–US has been evaluated by the degradation of textile dye, methylene blue in presence and absence of common inorganic salts (nitrate, acetate and sulphate). It was observed that in presence of anions the degradation of the dye increases significantly. The influence of the presence of H_2O_2 on the degradation rate was studied. The dependence of photodegradation of the dye rates on various parameters such as dye concentration, photocatalyst concentration and pH were also investigated. The photodegradation rate follows pseudo first order kinetics. H_2O_2 and UV light have a negligible effect in absence of Ti–Ag–US catalyst. The relative photonic efficiency of the system is reported using phenol as a standard organic compound.

Keywords: Photodegradation; Methylene blue; Sol–gel derived TiO_2; Silver doping; Common inorganic salts

1. Introduction

Dye pollutants from the textile industry are an important source of environmental contamination. It is estimated that from 1 to 15% of the dye is lost during dyeing processes and is released in waste waters [1]. The release of these colored waste waters in the eco system is a dramatic source of aesthetic pollution, eutrophication and perturbations in aquatic life [2].

A variety of physical, chemical and biological methods are presently available for treatment of textile waste water. Biological treatment is a proven technology and is cost effective. However, it has been reported that the majority of dyes are only adsorbed on the sludge and are not degraded [3]. Physical methods such as ion-exchange, adsorption, air stripping, etc., are also ineffective on pollutants which are not readily adsorbable or volatile, and have the further disadvantage that they simply transfer the pollutants to another phase rather than destroying them. This leads to search for highly effective method to degrade the dyes into environmentally compatible products. It has been revealed from the literature that photocatalysis can be used to destroy the dyes using semiconductor catalyst under light irradiation [4,5]. Among the semiconductors used, TiO_2 is considered particularly efficient owing to the formation of electron–hole pair under illumination with near UV light. The activity of titania is influenced by several factors such as crystallinity of the anatase phase [6,7], particle size, surface area [8,9] and the method of preparation [10,11]. It is known that the transformation from amorphous to anatase or rutile phase is influenced by the preparative experimental conditions [12]. Different preparation methods such as hydrolysis, sol–gel, microemulsion or reverse miscelles, hydrothermal and mechno chemical method [13] are

---

* Corresponding author. Fax: 91 422 2573833.
E-mail address: sspsgchemrp@yahoo.com (S. Senthilkumaar).

0143-7208/$ - see front matter © 2005 Elsevier Ltd. All rights reserved.
doi:10.1016/j.dyepig.2005.02.012

reported by several researchers [14–19] to synthesize nanoparticles of titania. The ultrasonication technique is extensively used for the preparation of mesoporous titania [20], anatase and rutile titania [21] and brookite titania [22], titania nanotubes [23] ZnO nano crystals [24], MCM-41 silica [25]. Several metals were used for doping especially Pt^0, Li^+, Zn^{2+}, Cd^{2+}, Mn^{2+}, Ce^{3+}, Cr^{3+}, Fe^{3+} and Al^{3+}. Platinization of titania has been proposed in early 1978 for the photocatalytic transformation of acetic acid [26]. The presence of transition metals may increase the photocatalytic activity by scavenging electrons that render the recombination of charges and favour the formation of hydroxyl radical. High concentration of metal (Cu^{2+}, Ni^{2+}) may have the detrimental effect either by competitive trapping of oxidizing species h^+ and $OH^\bullet$ or by filter effect when salts significantly absorbed in UV range. Besides the redox potentials of Cu/Cu^+, Cu^+/Cu^{2+} and Fe^{2+}/Fe^{3+} permit the formation of photocurrent. With Pt and Pd salts deposition of Pt^0 and Pd^0 may occur on the particles of TiO_2 [27]. Okamoto et al. [28] reported that the influence of Ce^{2+} may be positive or negative according to the concentration. Kiriakidodu et al. [29] reported that the addition of Ca^{2+} to titanium significantly decreases the photocatalytic decomposition of acid orange 7, whereas the presence of W^{6+} has a significant positive effect for the small per cent of W^{6+}. It is believed that different processes may be involved according to experimental conditions hence it is difficult to assess the influence of transition metal on photocatalysis and experiments are necessary to point out the effect of these metals.

In this present work, we report on the novelty of ultrasonication technique coupled with sol–gel method for the synthesis of nanocrystalline single phase pure anatase titania doped with silver (Ti–Ag–US) at room temperature while others have reported mixed phases [15,21]. The influence of this irradiated photocatalyst on the degradation of MB in aqueous system was reported. Its structure is presented in Fig. 1. The parameters studied include irradiation time, effect of initial MB concentration, concentration of nanocrystalline Ti–Ag–US, effect of H_2O_2, effect of common inorganic salts and pH.

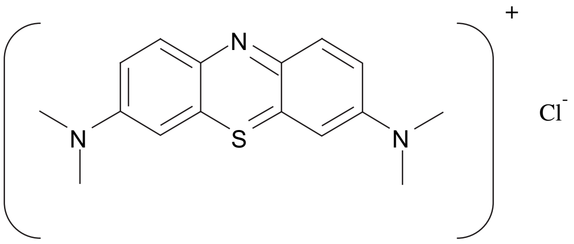

Fig. 1. Structure of methylene blue.

2. Materials and methods

2.1. Chemicals

Titanium (IV) *n*-butoxide (99%) was purchased from Lancaster and used as such. Analar grade glacial acetic acid and *n*-butanol were obtained from SD's Fine Chemicals and were triply distilled. The analar quality sodium salt of NO_3^-, SO_4^{2-}, acetate, H_2O_2 (100 volumes), Silver nitrate and dye methylene blue (MB) were procured from SD's Fine Chemicals and used as received.

2.2. Synthesis of nanocrystalline TiO_2

The experimental flow chart for the synthesis of TiO_2 bulk is given in Fig. 2. Detailed procedure for the preparation of TiO_2 is discussed as follows: titanium (IV) *n*-butoxide (3.5 g) is added to 4 g of glacial acetic acid with constant stirring. To the reaction mixture, *n*-butanol (42.5 g) and silver nitrate (0.1 N) are added slowly. The total volume of the reactants is maintained to be 100 ml. The contents are stirred vigorously for 6–8 h. The excess solvent is evaporated by drying in a vacuum air oven at 150 °C for 12 h. The TiO_2 sol obtained was ultrasonically treated for 30 min. The derived gel is subjected to calcination at 500 °C for 30 min and labeled Ti–Ag–US. The final product is ground to get fine particles. In case of titanium alkoxide precursors, dilute solutions of the reactants, i.e., water (hydroxyl group precursor) and alkoxide (titanium precursor) in excess ethanol allow physical separation of the reactants. But titanium butoxide is extremely water sensitive precursor. Therefore, the maximum titania loading that can be achieved without second phase precipitation of titania is limited. In general, as the loading of the dispersed phase is increased we can see the precipitation of a second phase [30]. The XRD pattern of Ti–Ag–US was recorded on Schimadzu X-Ray diffractometer over a 2θ range of 20–80° with a step size of 0.02° and a collection time of 0.3 s ($\lambda = 1.541$). The strongest peak at $2\theta = 25.2°$ is representative for (101) anatase phase reflections, where by applying the Scherrer's formula, the Ti–Ag–US crystallites size can be estimated at 44 nm [31].

2.3. Photocatalytic decomposition of methylene blue

Experiments were performed in an open thermostated pyrex reactor of 250 ml capacity and provided with water circulation arrangement in order to maintain the temperature. The suspensions in the reactor were left for 60 min in dark in order to achieve the maximum adsorption of the dye on to Ti–Ag–US surface. The irradiation was carried out using 125 W (311 nm) medium pressure Hg arc lamp. The average light

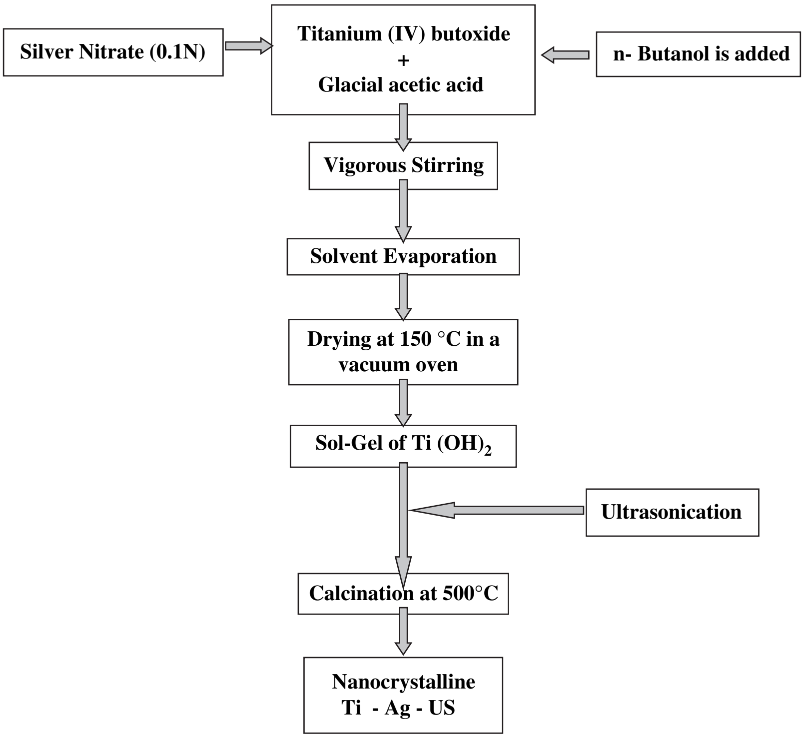

Fig. 2. Synthesis of nanocrystalline TiO_2–Ag.

intensity on the reaction vessel at a distance of 15 cm from the lamp was found to be 1.6×10^{-4} Einstein $\min^{-1}$.

In all the studies, 150 ml of MB solution containing an appropriate amount of Ti–Ag–US was magnetically stirred, before and during illumination. At specific time intervals, 5 ml of the sample was withdrawn and filtered through 0.45 μm filters. Changes in the concentration of MB were observed from its characteristic absorption at 666 nm using a UV–vis spectrophotometer (Schimadzu UV-1601). The influences of (0.025 M) anions such as nitrate, sulphate and acetate on the photodegradation of MB (10 mg/L) in presence of Ti–Ag–US (330 mg/L) at pH (6.80) were studied. All experiments, except were otherwise mentioned in the text, were carried out at natural pH (6.80).

3. Results and discussion

3.1. Adsorption isotherm

Adsorption tests in dark conditions were carried out in order to evaluate the equilibrium constants of the adsorption of dye on the TiO_2 surface at different concentrations. The extent of equilibrium adsorption was determined from the decrease in dye concentration. The amount of dye molecules adsorbed on Ti–Ag–US was determined by Eq. (1) [32],

$$n = \frac{V \Delta C}{W} \tag{1}$$

where n is the number of dye molecules adsorbed per gram of Ti–Ag–US, ΔC the decrease in the dye concentration in mg/L, W the weight of Ti–Ag–US in grams and V is the volume of dye solution in litre. The value of $n_{\max}$ for the equilibrium of adsorption of MB was calculated as 5.61 mg/g from the following Eq. (2),

$$\frac{C_{eq}}{n} = \frac{1}{K n_{\max}} + \frac{C_{eq}}{n_{\max}} \tag{2}$$

where n is the number of adsorption sites on Ti–Ag–US, C_{eq} is the equilibrium concentration of dye and K is the equilibrium constant for MB adsorption.

3.2. Change of absorption spectra

Fig. 3 shows the change in absorption spectrum of 10 ppm MB on irradiation in an aqueous solution containing 0.125 mg/L Ti–Ag–US. The absorption spectrum is seen to decrease in intensity with increase in irradiation time. The rapid decrease in the intensity of 666 nm band in Fig. 3 suggests that the chromophore responsible for characteristic color of the MB is breaking down.

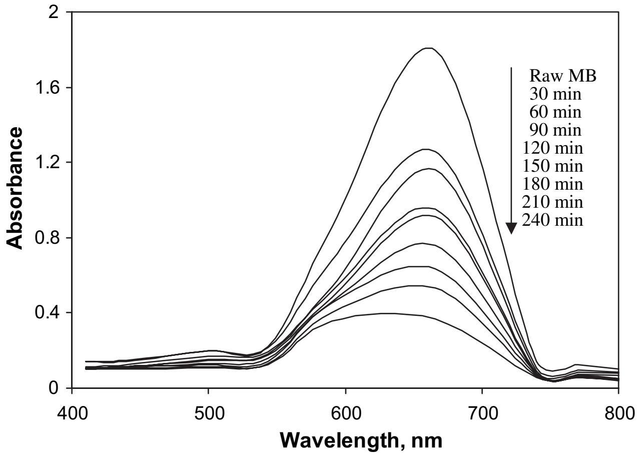

Fig. 3. Change of absorption spectra of MB with irradiation time.

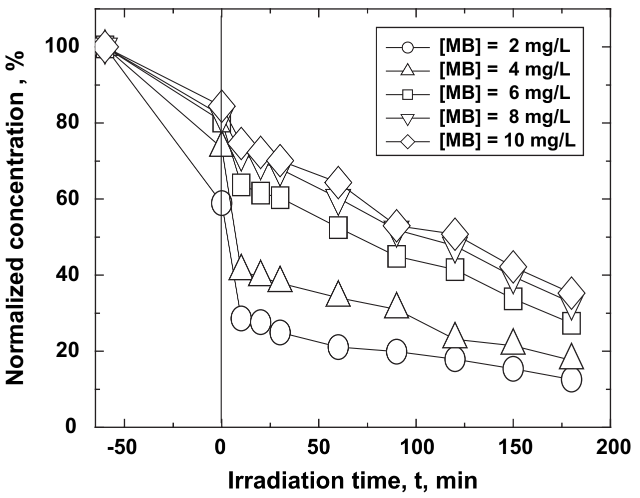

Fig. 4. Effect of initial concentration and irradiation time on MB degradation. Conditions: [Ti–Ag–US] = 333 mg/L; pH = 6.80.

3.3. Effect of initial MB concentration and irradiation time

Fig. 4 shows the normalized concentration vs. irradiation time for different initial MB concentrations at fixed Ti–Ag–US concentration. The experimental kinetic data follow the pseudo first order kinetic expression, which is rationalized in terms of the Langmuir–Hinshelwood model modified to accommodate reactions occurring at a solid–liquid interface [33,34].

$$r_0 = -\frac{\mathrm{d}c}{\mathrm{d}t} = \frac{k_\mathrm{r} K C_\mathrm{eq}}{1 + K C_\mathrm{eq}} \tag{3}$$

where r_0 is the initial rate of disappearance of the organic substrate and C_eq is the equilibrium bulk solute concentration. K represents the equilibrium constant for adsorption of the organic substrate onto Ti–Ag–US and k_r reflects the limiting rate of reaction at maximum coverage under the given experimental conditions. This equation can be used when the data demonstrate linearity when plotted as follows:

$$\frac{C_\mathrm{eq}}{r_0} = \frac{1}{k_\mathrm{r} K} + \frac{C_\mathrm{eq}}{k_\mathrm{r}} \tag{4}$$

The photodecomposition of various initial concentrations of MB in the presence of fixed amount of Ti–Ag–US is illustrated in Fig. 4, which depicts the distinction equilibrium between the dark adsorption–desorption equilibrium and the additional decrease in MB concentration caused by UV illumination. From Fig. 4 it is clear that MB is adsorbed strongly on Ti–Ag–US. For this reason, the equilibrium concentration of the CV dye (C_eq), instead of the initial one, has been used in the kinetic study [35,36]. The k_r and K values were calculated from the slope and the intercept of C_eq/r_0 vs. C_eq plot (Fig. 5) and found to be 0.0199 mg/L min and 0.3689 L/mg, respectively.

3.4. Effect of catalyst concentration

Experiments were carried out with different concentrations of catalyst (0.200–0.533 g/L) at fixed MB concentration (10 mg/L). It has been observed that the initial rate increases with an increase in the amount of catalyst and that it remains almost constant above a certain level and is presented in Table 1. This has been explained as the concentration of the catalyst is increased; the number of photons absorbed and the number of dye molecules adsorbed are increased with respect to an increase in the number of catalyst

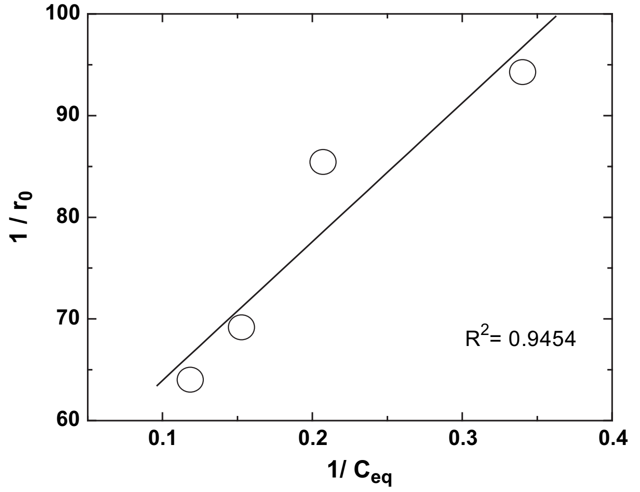

Fig. 5. Kinetics of photocatalytic MB degradation. Conditions: [Ti–Ag–US] = 333 mg/L; pH = 6.80.

Table 1
Effect of Ti–US concentration on the decolorization rate

$[TiO_2]$ (g/L)	r_0 (mg/L min)
0.200	0.0517
0.267	0.0630
0.333	0.0920
0.400	0.2193
0.533	0.3147

molecules. The density of the molecule in the area of illumination also increases and thus the rate gets enhanced. After a certain level, the dye molecules available are not sufficient for adsorption by the increased number of catalyst molecule. Hence, the additional catalyst powder is not involved in the photocatalytic activity and the rate does not increase with increase in the amount of catalyst beyond certain limit. It is also expected that the aggregation of the catalyst molecules at high concentration must also be considered, which causes the decrease in the number of active surface sites. The experimental data are found in good agreement with those reported by Sauer et al. [37] for the degradation of Safira dye using Degussa P-25. Neppolian et al. [38] also reported the decreased per cent degradation of reactive dyes at higher catalyst concentration. Further, it is explained that the deactivation of activated molecule by collision with the ground state molecule with the shielding of TiO_2 may also take place according to Eq. (5),

$$\text{Ti–Ag–US}^{*} + \text{Ti–Ag–US} \rightarrow \text{Ti–Ag–US}^{\bullet} + \text{Ti–Ag–US} \tag{5}$$

where Ti–Ag–US* is the Ti–Ag–US with active species adsorbed in its surface and Ti–Ag–US$^\bullet$ the deactivated form of Ti–Ag–US. Hence, an optimum catalyst concentration has to be maintained to ensure total absorption of photons for efficient photodegradation [39].

Galindo et al. [1] reported an empirical initial degradation rate and catalyst concentration as $r_0 \propto [TiO_2]^n$ [dye] where n is the exponent less than one for the dye studied in reaction to the lower concentration of catalyst. In our present work, the initial degradation rate follows a similar relationship and the 'n' value was found to be 2.05 when the Ti–Ag–US concentration was less than 1.0 g/L (Fig. 6).

3.5. Effect of pH

The influence of pH on the decolorization of MB is shown in Fig. 7. The results showed that there was a strong dependence of pH of the solution on the heterogeneous photoprocess. It is known that the metal oxide particles suspended in water behave similar to diprotic acids. For TiO_2, hydroxyl groups undergo two acid base equilibria:

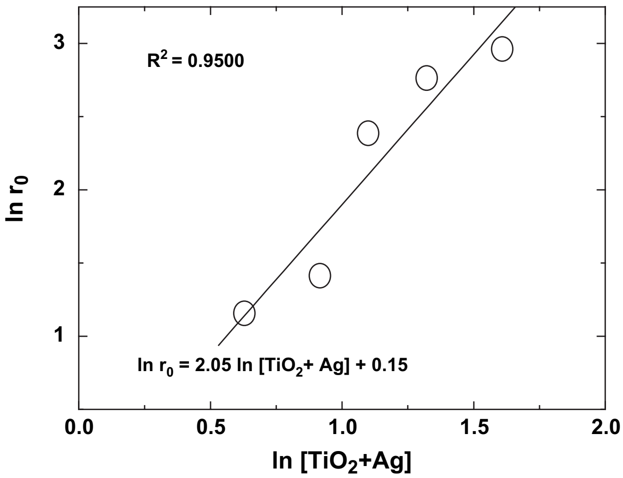

Fig. 6. Effect of catalyst concentration on MB degradation rate. Conditions: [MB] = 10 mg/L; pH = 6.80.

$$>TiOH_2^+ \leftrightarrow >TiOH + H^+ \tag{6}$$

$$>TiOH \leftrightarrow >TiO^- + H^+ \tag{7}$$

Generally, for charged substrates, a significant dependency of the photocatalytic degradation efficiency on pH value had been observed, since the overall surface charge and hence the adsorptive properties of TiO_2 particles depend strongly on solution pH [40,41].

In our experiments, any changes in initial degradation rate with varying pH values must be ascribed to variations of the acid/base properties of the Ti–Ag–US particle surface (Eqs. (6) and (7)). Since the photooxidation of dyes is accompanied by the release of protons

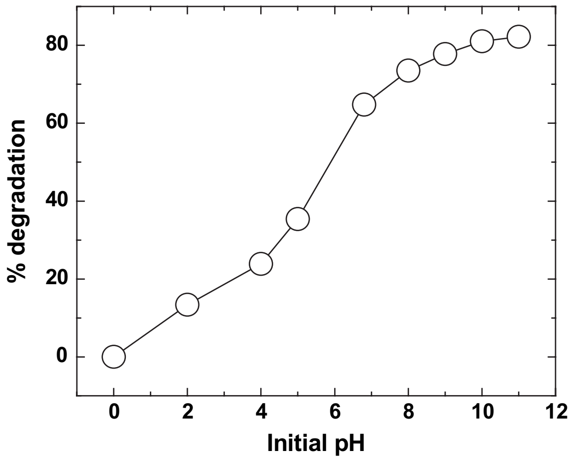

Fig. 7. Effect of initial pH on MB degradation. Conditions: [MB] = 10 mg/L; [Ti–Ag–US] = 333 mg/L; irradiation time = 3 h.

[42], its efficiency may then change because of the reversible protonation of the Ti–Ag–US surface. The MB is a cationic dye in aqueous solution. In acidic pH range (pH < 6.8), Ti–Ag–US acquires positive charge and hence electrostatic repulsion between Ti–Ag–US and dye cation retards the degradation rate. On the other hand, in basic pH (pH > 6.8), electrostatic interaction between the negative Ti–Ag–US and dye cation leads to strong adsorption with the corresponding high rate of degradation and reaches a maximum at pH 10. This behaviour is characteristics for many photocatalytic systems and similar results have been reported by the photodegradation of other dyes [42].

3.6. Effect of H_2O_2 on the photodegradation of MB

Experiments were conducted to evaluate the effect of H_2O_2 on the MB photodegradation (Fig. 8). In our study, photocatalytic efficiency increases as the concentration of H_2O_2 increases and reaches optimum at 3.4 mg/L and further increases in concentration up to 6.8 mg/L leading to decrease in the photodegradation rate. The addition of H_2O_2 increases the concentration of $OH^{\bullet}$ radical since it inhibits the e^-, h^+ recombination according to the Eq. (8),

$$TiO_{2(e^-)} + H_2O_2 \rightarrow TiO_2 + OH^- + OH^{\bullet} \tag{8}$$

H_2O_2 is considered to have two functions in the photocatalytic degradation. It accepts a photogenerated conduction band electron thus promotes the charge separation (Eq. (9)) and it also forms $OH^{\bullet}$ (Eq. (10)).

$$H_2O_2 + e^- \rightarrow OH^- + OH^{\bullet} \tag{9}$$

$$H_2O_2 + O_2^{-\bullet} \rightarrow OH^- + OH^{\bullet} + O_2 \tag{10}$$

The addition of H_2O_2 is a well known mechanism to increase the rate of photocatalytic degradation with higher quantum yield of formation of $OH^{\bullet}$ [43,44]. Consequently, the degradation rate is expected to be increased. Further increase of H_2O_2 after the quantum level, decreases the rate of degradation slowly. This negative effect of high concentration of H_2O_2 may be due to the formation of $OH_2^{\bullet}$. When the H_2O_2 concentration is higher, $OH_2^{\bullet}$ formed is significantly less reactive than $OH^{\bullet}$. Wang and Hong [45] reported that the H_2O_2 on the catalyst surface acts as a powerful $OH^{\bullet}$ scavenger (Eqs. (11) and (12)) along with a photogenerated holes (Eq. (14)) and thus inhibits the generation of $OH^{\bullet}$ radical and thereby decreases the degradation rate.

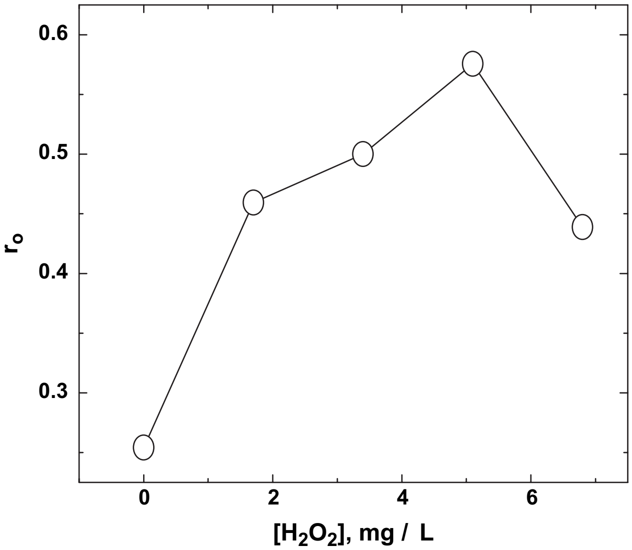

Fig. 8. Effect of H_2O_2 on MB degradation. Conditions: [MB] = 10 mg/L; [Ti–Ag–US] = 0.25 mg/L; pH = 10.0.

$$H_2O_2 + OH^{\bullet} \rightarrow H_2O + HO_2^{\bullet} \tag{11}$$

$$HO_2^{\bullet} + OH^{\bullet} \rightarrow H_2O + O_2 \tag{12}$$

$$H_2O_2 + h_{vb}^{+} \rightarrow HO_2^{\bullet} + H^+ \tag{13}$$

Several researchers have reported the beneficial effect of H_2O_2 on the photocatalytic degradation of pesticides [46,47], benzene, organo phosphorous derivatives, organo halides and dioxins [48,49], whereas a negative effect has also been reported by Chemsedine and Bohem [50] for the degradation of chloro acid on TiO_2.

3.7. Effect of inorganic salts

The effect of inorganic salts on the degradation process was investigated with common inorganic salts such as nitrate, sulphate and acetate (0.025 M). As can be seen from the Fig. 9, the effectiveness of Ti–Ag–US system was significantly increased in presence of anion. The order of reactivity towards the decomposition of MB was found to be acetate > nitrate > sulphate. Adsorption of MB on TiO_2 was significantly increased in presence of anion species. It can be explained as the reaction of the positive hole (h^+) formed on the Ti–Ag–US with anions and those anions behave like h^+ scavengers resulting prolonged color removal in 0–30 min irradiation. Probably, the adsorbed anions compete with the dye for the photooxiding species on

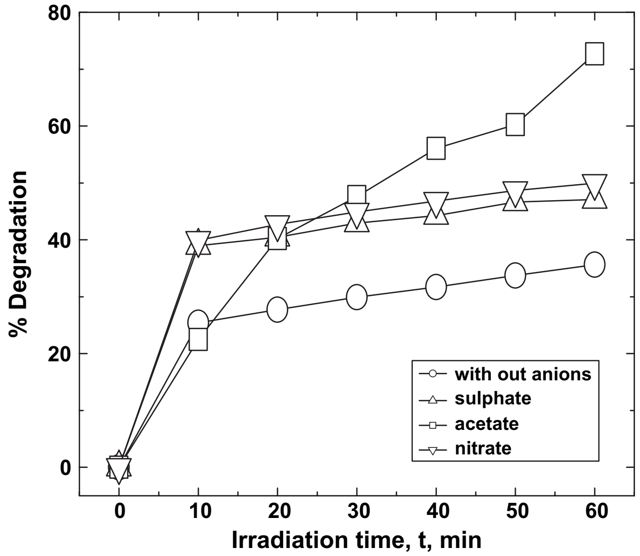

Fig. 9. Effect of common inorganic salts on MB degradation. Conditions: [MB] = 10 mg/L; [inorganic salt] = 250 mg/L; [Ti–Ag–US] = 0.250 mg/L; pH = 6.80.

the surface to form oxidizing inorganic radicals. It is expected that the recombination of h^+ and the electron will be prohibited by these anions leaving the electron for the photodecomposition of MB. It is also expected that some of these radical anions react with the chromophoric groups of surface adsorbed dye and may enhance the rate of degradation. The observed effect is still thought to be strong adsorption of anions on Ti–Ag–US surface [51,52].

3.8. Calculation of relative photonic efficiency

In order to compare the degradation and efficiency of Ti–Ag–US, the relative photonic efficiency (ξ_r) was calculated using Eq. (14).

$$\xi_r = \frac{\text{Rate of disappearance of dye}}{\text{Rate of disappearance of phenol}} \tag{14}$$

where both (initial) the rates are obtained under exactly the same condition. The relative photonic efficiency of the dye degradation is 4.05. The efficiency is greater than unity, indicating that the initial photocatalysed oxidative degradation of the dye is more efficient than for phenol [53].

4. Conclusions

- Nanocrystalline, pure anatase titania doped with silver (Ti–Ag–US) was prepared by sol–gel process via ultrasonic irradiation.
- The average crystallite size calculated from Debye–Sherrer equation was found to be 44 nm.
- It was observed that Ti–Ag–US is efficient for the degradation of MB from aqueous solution.
- From the experimental results, the dependence of the Ti–Ag–US concentration on the initial decolorization rate follows a relationship, $r_0 \propto [TiO_2]^n$. The value of n was found to be 2.05.
- The photocatalytic rate of MB increased in presence of H_2O_2.
- The influence of H_2O_2 on the decomposition rate reveals the fact that the most possible oxidation mechanism of MB is the dual hole–radical mechanism.
- The optimum concentration of 5 mg/L of H_2O_2 is required for the effective degradation of 10 mg/L of MB at pH 10.
- The experimental data suggest that the degradation of MB follows pseudo first order kinetics.
- The sol–gel coupled with ultrasonic technique is fast and gives uniform distribution of crystallites of pure anatase titania confirmed by XRD studies.
- Ultrasonication does not only reduce the crystallite size but also enhances the hydrolysis of titanium alkoxide for faster and better crystallization of anatase nano particles.
- From the result of present work and the literature, one could understand that photocatalytic treatment of textile industry waste-water is a promising tool for the decolorization of colored wastewaters.

References

[1] Galindo C, Jacques P, Dalt A. Photooxidation of the phenylazonaphthol AO20 on TIO_2: kinetic and mechanistic investigations. Chemosphere 2001;45:997–1005.

[2] Herrmann JM, Vautier M, Guillard C. Photocatalytic degradation of dyes in water: case study of indigo and of indigo carmine. J Catal 2001;201:46–59.

[3] Pagga U, Taeger K. Development of a method for adsorption of dyestuffs on activated sludge. Water Res 1994;28:1051–7.

[4] Hoffmann MR, Martin ST, Choi W, Bahnemann DW. Environmental applications of semiconductor photocatalysis. Chem Rev 1995;95:69–96.

[5] Neppolian B, Sakthivel S, Palanichamy M, Arabindoo B, Murugasen V. Photocatalytic degradation of textile dye commonly used in cotton fabrics. Stud Surf Sci Catal 1998; 113:329–35.

[6] Nishimoto SI, Ohtani B, Hajiwara H, Kagiya T. Correlation of the crystal structure of titanium dioxide prepared from titanium tetra-2-propoxide with the photocatalytic activity for redox reactions in aqueous propan-2-ol and silver salt solutions. J Chem Soc Faraday Trans I 1985;81:61–8.

[7] Fox MA, Dulay MT. Heterogeneous photocatalysis. Chem Rev 1993;93:341–57.

[8] Zhang Z, Wang CC, Zakaria R, Ying JY. Role of particle size in nanocrystalline TiO_2 based photocatalysts. J Phys Chem B 1998;102:10871–8.

[9] Zhang H, Penn RL, Hamers RJ, Banfield JF. Enhanced adsorption of molecules on surfaces of nanocrystalline particles. J Phys Chem B 1999;103:4656–62.

[10] Reddy KM, Gopal Reddy CV, Manorama SV. Preparation, characterization, and spectral studies on nanocrystalline anatase TiO_2. J Solid State Chem 2001;158:180–6.

[11] Wang CC, Ying JY. Sol–gel synthesis and hydrothermal processing of anatase and rutile titania nanocrystals. Chem Mater 1993;11:3113–20.

[12] Madhu Kumar P, Badrinarayann S, Sastry Murali. Nanocrystalline TiO_2 studied by optical, FT-IR and X-ray photo electron spectroscopy. Correlation to presence of surface states. Thin Solid Films 2000;358:122–30.

[13] Yin Shu, Zhang Qiwu, Saito Fumio, Sato Tsugio. Preparation of visible light-activated titania photocatalyst by mechanochemical method. Chem Lett 2003;32:358–9.

[14] Vigil E, Ayllon JA, Peiro AM, Clemente RR. TiO_2 layers grown from flowing precursor solutions using microwave heating. Langmuir 2001;17:891–6.

[15] Zhang H, Finnegan M, Banfield JF. Preparing single phase nanocrystalline anatase from amorphous titania with particle sizes tailored by temperature. Nano Lett 2001;1:81–5.

[16] Scolan E, Sanchez C. Synthesis and characterization of surface-protected nanocrystalline titania particles. Chem Mater 1998;10:3217–23.

[17] Chhabra V, Pillai V, Mishra BK, Morrone A, Shah DO. Synthesis and characterization and properties of microemulsion-mediated nanophase TiO_2 particles. Langmuir 1995;11: 3307–11.

[18] Stathatos E, Lianos P, Del Monte FV, Levy D, Tsiourvas D. Formation of TiO_2 nanoparticles in reverse micelles and their deposition as thin films on glass substrates. Langmuir 1997;13:4295–300.

[19] Wu XM, Wang L, Tan ZC, Li GH, Qu SS. Preparation, characterization, and low-temperature heat capacities of nanocrystalline TiO_2 ultrafine powder. J Solid State Chem 2001;156:220–4.

[20] Wang YQ, Chen SG, Tang XH, Palchik O, Zaban A, Koltypin Y, et al. Mesoporous titanium dioxide: sonochemical synthesis and application in dye-sensitized solar cells. J Mater Chem 2002;11:521–6.

[21] Huang W, Tang X, Wang Y, Koltypin Y, Gedanken A. Selective synthesis of anatase and rutile via ultra sonic irradiation. Chem Commun 2000;1415–6.

[22] Yu JC, Vu J, Ho W, Zhang L. Preparation of highly photocatalytic active nano-sized TiO_2 particles vis ultrasonic irradiation. Chem Commun 2001;1942–3.

[23] Zhu Y, Li H, Koltypin Y, Hacohen YR, Gedanken A. Sonochemical synthesis of titania whispers and nonotubes. Chem Commun 2001;2616–7.

[24] Qian Dong, Jiang JZ, Lenvig Hansen Poul. Preparation of ZnO nanocrystals via ultrasonic irradiation. Chem Commun 2003;1078–9.

[25] Tang Xianghai, Liu Suwen, Wang Yanqin, Huang Weiping, Sominski Elena, Palchik Oleg, et al. Rapid synthesis of high quality MCM-41 silica with ultrasonic irradiation. Chem Commun 2000;2119–20.

[26] Kraeulter B, Bard AJ. Heterogeneous photocatalytic decomposition of saturated carboxylic acids on TiO_2 powder. Decarboxylative route to alkanes. J Am Chem Soc 1978; 100:5985–92.

[27] Litter MI. Heterogeneous photocatalysis: transition metal ions in photocatalytic systems. Appl Catal B 1999;23:89–114.

[28] Okamoto K, Yamamoto Y, Tanaka H, Tanaka M, Itaya A. Heterogeneous photocatalytic decomposition of phenol over TiO_2 powder. Bull Chem Soc Jpn 1985; 58:2015–22.

[29] Kiriakidodu F, Kondarides DI, Verykios XE. The effect of operational parameters and TiO_2-doping on the photocatalytic degradation of azo-dyes. Catal Today 1999;54:119–30.

[30] Hanprasopwattana A, Reiker Thomas, Sault Allen G, Datye AK. Morphology of titania coatings on silica gel. Catal Lett 1997;45:165–75.

[31] Awati PS, Awate SV, Shah PP, Ramaswamy V. Photocatalytic decomposition of methylene blue using nanocrystalline anatase titania prepared by ultrasonic technique. J Photochem Photobiol A 2003;4:393–400.

[32] Parra S, Olivero J, Pulgarin C. Relationships between physicochemical properties and photo reactivity of four biorecalcitrant phenylurea herbicides in aqueous TiO_2 suspension. Appl Catal B 2002;36:75–85.

[33] Turchi CS, Ollis DF. Photocatalytic degradation of organic water contaminants: mechanisms involving hydroxyl radical attack. J Catal 1990;122:178–92.

[34] Al Ekabi H, Serpone N. Kinetic-studies in heterogeneous photocatalysis. 1. Photocatalytic degradation of chlorinated phenols in aerated aqueous solutions over TiO_2 supported on glass matrix. Phys Chem 1988;92:5726–31.

[35] Zhang F, Zhao J, Shen T, Hidaka H, Pelizzetti E, Serpone N. TiO_2-assisted photodegradation of dye pollutants II. Adsorption and degradation kinetics of eosin in TiO_2 dispersions under visible light irradiation. Appl Catal B 1998;15:147–56.

[36] Matthews RW, Abdullah M, Low GK. Photocatalytic oxidation of total organic analysis. Anal Chem Acta 1990;233:171–9.

[37] Sauer T, Cesconeto Neto G, Jose HJ, Moreira RFPM. Kinetics of photocatalytic degradation of reactive dyes in a TiO_2 slurry reactor. J Photochem Photobiol A 2002;149:147–54.

[38] Neppolian B, Sakthivel S, Palanichamy M, Arabindoo B, Murugasen V. Solar/UV-induced photocatalytic degradation of three commercial textile dyes. J Hazard Mater B 2002;89:303–17.

[39] Herrmann JM. Heterogeneous photocatalysis: an emerging discipline involving multiphase systems. Catal Today 1995;24:157–64.

[40] Tang WZ, An H. UV/TiO_2 photocatalytic oxidation of commercial dyes in aqueous solutions. Chemosphere 1995;31:4157–70.

[41] Wang K, Hisieh Y, Wu C, Chang C. The pH and anion effects on the heterogeneous photocatalytic degradation of *o*-methylbenzoic acid in TiO_2 aqueous suspension. Chemosphere 2000;40:389–94.

[42] Poulios I, Tsachpinis I. Photodegradation of the textile dye reactive black 5 in the presence of semiconducting oxides. J Chem Technol Biotechnol 1999;71:349–57.

[43] Hachem C, Bocquillon F, Zahraa O, Bouchy M. Decolourization of textile industry wastewater by the photocatalytic degradation process. Dyes Pigments 2001;49:117–25.

[44] Salvador P, Decker F. The generation of hydrogen peroxide during water photo electrolysis at *n*-titanium dioxide. J Phys Chem 1984;88:6116–20.

[45] Wang Y, Hong CS. Effect of hydrogen peroxide, periodate and persulfate on photocatalysis of 2-chlorobiphenyl in aqueous TiO_2 suspensions. Water Res 1999;33:2031–6.

[46] Mengyne Z, Shifu C, Yaowu T. Photocatalytic degradation of organo phosphorous pesticides using thin film of TiO_2. J Chem Technol Biotechnol 1995;64:339–44.

[47] Weichgrebe D. Beitrag Zur Chemison – oxidativen abwasserbehandlung. Ph.D. dissertation. TUClausthal, Germany; 1994.

[48] Wolfrum E, Ollis D. Hydrogen peroxide in hetrogeneous photocatalysis; 1994. p. 451–65 [chapter 32].

[49] Tanaka K, Hisanaga T, Harada K. Photocatalysis degradation of organohalides compounds in semi conductive suspension with added hydrogen peroxide. New J Chem 1989;13:5.

[50] Chemsedine A, Bohem HP. A study of the primary step in the photochemical degradation of acetic acid and chloro acetic acids on a TiO_2 photocatalyst. J Mol Catal 1990;60:295–311.

[51] Abdullah M, Low C, Mathews RW. Effects of common inorganic anions on rates of photocatalytic oxidation of organic

carbon over illuminated titanium dioxide. J Phys Chem 1990; 94:6820–5.

[52] Bekbolet M, Boyacioglu Z, Ozkaraova B. The influence of solution matrix on the photocatalytic removal of color from natural waters. Water Sci Technol 1998;38:155–62.

[53] Serpone N, Sauve G, Koch R, Tahiri H, Pichat P, Pelizzetti E, et al. Standardization protocol of process efficiencies and activation parameters in heterogeneous photocatalysis: relative photonic efficiencies ζ_r. J Photochem Photobiol A 1996;94: 191–203.